New Metallodendrimers Containing an Octakis(diphenylphosphino)-Functionalized Silsesquioxane Core and Ruthenium(II)-Based Chromophores

Hunter J. Murfee, Travis P. S. Thoms,† John Greaves, and Bo Hong*

Department of Chemistry, 516 Rowland Hall, University of California, Irvine, California 92697-2025

Received May 5, 2000

A new class of surface-modified dendrimers has been prepared by reactions of 8 equiv of the terpyridine-functionalized polyether monodendrons with a polyhedral oligomeric silsesquioxane (POSS) core. Subsequent reactions of these spherically shaped organic dendrimers with Ru(II)-based precursors afford photo- and redox-active metallodendrimers. These new dendrimers have been characterized using a combination of mass spectral analysis (MALDI-TOF/MS, ESI/MS, and FAB/MS), nuclear magnetic resonance (^{1}H, ^{13}C, ^{29}Si, and ^{31}P{^{1}H} NMR), photophysical analyses (electronic absorption, emission, excited-state lifetime, and quantum yield) and electrochemical measurement (cyclic voltammetry). Specifically, ^{31}P{^{1}H} NMR is used to monitor the completion of reactions and the purity of dendrimers and metallodendrimers. These new metallodendrimers exhibit large extinction coefficients that coincide with the number of peripheral Ru(II)-based chromophores. With the use of (-CH_2-Ph-tpy)$Ru^{II}(bpy)_2$ type of chromophores, all metallodendrimers are found emissive at room temperature, with lifetimes in the range of 605−890 ns. Photophysical data also indicate similar steady-state emission maxima and single-exponential decay kinetics for all metallodendrimers, and the observed overall quantum yields of the G1, G2, and G3 metallodendrimers are found to be 14, 20, and 7 times higher than that of the monomeric model complex (CH_3-Ph-tpy)Ru$(bpy)_2(PF_6)_2$. Electrochemical studies reveal the presence of surface-confined species, in addition to the ligand-centered and metal-centered redox processes.

Introduction

The study of new supramolecular and polymeric systems with the ability to perform complex functions has received increasing interests in recent years.[1−9] Of the systems that are currently under investigation, dendrimers and metallodendrimers are promising.[1−3] Photoactive, redox-active, and/or catalytically active organometallic moieties can be incorporated into any component[3a,3e,4] of a dendrimer, including the branching points,[5] core,[6] and periphery,[3b,3f,7] to give metallodendrimers with desired functionality. These metallodendrimers combine the unique properties of transition metals, such as redox properties and photoactivity, to the already diverse characteristics of dendrimers, yielding highly functionalized molecular systems.[3−7] The ability to control the structural and chemical compositions of dendrimers and metallodendrimers renders them applicable to diverse applications such as solar energy conversion,[1a,3a,6c,8] photomolecular devices,[1a] molecular electronics,[1b] and information storage.[1a,b]

We are interested in the construction and characterization of metallodendrimers with a central silsesquioxane core and multiple surface-confined Ru(II)-based chromophores, Figure 1. Polyhedral oligomeric silsesquioxane serves as an inert and

* To whom correspondence should be addressed. E-mail: BHONG@uci.edu. Fax: (949)-824-3168.

† Currently at Gemfire Corp., Palo Alto, CA.

(1) Balzani, V.; Scandola, F. *Supramolecular Photochemistry*; Ellis Horwood: New York, 1991. (b) Carter, F. L.; Siatkowski, R. E.; Wohltjen, H. *Molecular Electronic Devices*; North-Holland: Amsterdam, 1988. (c) Sauvage, J. P.; Collin, J. C.; Chambron, J. C.; Guillerez, S.; Coudret, C.; Balzani, V.; Barigelletti, F.; Decola L.; Flamigni, L. *Chem. Rev.* **1994**, *94*, 993−1019. (d) Fox, M. A. *Acc. Chem. Res.* **1999**, *32*, 201−207. (e) Astruc, D. *Acc. Chem. Res.*, in press. (f) Zeng, F. W.; Zimmerman, S. C. *Chem. Rev.* **1997**, *97*, 1681−1712. (g) Bosman, A. W.; Janssen, H. M.; Meijer, E. W. *Chem. Rev.* **1999**, *99*, 1665−1688. (h) Matthews, O. A.; Shipway, A. N.; Stoddart, J. D. *Prog. Polym. Sci.* **1998**, *23*, 1−56.

(2) Fréchet, J. M. J. *Science* **1994**, *263*, 1710−1715. (b) Tomalia, D. A. *Adv. Mater.* **1994**, *6*, 529−539. (c) Tomalia, D. A. *Sci. Am.* **1995**, 62−66. (d) Wooley, K. L.; Hawker, C. J.; Fréchet, J. M. J. *J. Am. Chem. Soc.* **1993**, *115*, 11496−11505.

(3) Balzani, V.; Campagna, S.; Denti, G.; Juris, A.; Serroni, S.; Venturi, M. *Acc. Chem. Res.* **1998**, *31*, 26−34. (b) Storrier, G. D.; Takada, K.; Abruña, H. D. *Langmuir* **1999**, *15*, 872−884. (c) Gorman, C. *Adv. Mater.* **1998**, *10*, 295−309. (d) Newkome, G. R.; He, E. F.; Moorefield, C. N. *Chem. Rev.* **1999**, *99*, 1689−1746. (e) Constable, E. C. *Chem. Commun.* **1997**, 1073−1080. (f) Valério, C.; Alonso, E.; Blais, J.-C.; Astruc, D. *Angew. Chem., Int. Ed. Engl.* **1999**, *38*, 1747−1751. (g) Alonso, E.; Astruc, D. *J. Am. Chem. Soc.* **2000**, *122*, 3222−3223. (h) Lange, P.; Schier, A.; Schmidbaur, H. *Inorg. Chem.* **1996**, *35*, 637−642. (i) Nlate, S.; Ruiz, J.; Blais, J.-C.; Astruc, D. *Chem. Commun.* **2000**, 417−418.

(4) Constable, E. C.; Harverson, P.; Oberholzer, M. *Chem. Commun.* **1996**, 1821−1822.

(5) Achar, S.; Vittal, J. J.; Puddephatt, R. J. *Organomet.* **1996**, *15*, 43−50.

(6) Kawa, M.; Fréchet, J. M. J. *Chem. Mater.* **1998**, *10*, 286−296. (b) Vogtle, F.; Plevoets, M.; Nieger, M.; Azzellini, G. C.; Credi, A.; De Cola, L.; De Marchis, V.; Venturi, M.; Balzani, V. *J. Am. Chem. Soc.* **1999**, *121*, 6290−6298. (c) Issberner, J.; Vogtle, F.; DeCola, L.; Balzani, V. *Chem. Eur. J.* **1997**, *3*, 706−712. (d) Cardona, C. M.; Kaifer, A. E. *J. Am. Chem. Soc.* **1998**, *120*, 4023−4024. (e) Gorman, C. B.; Parkhurst, B. L.; Su, W. Y.; Chen, K. Y. *J. Am. Chem. Soc.* **1997**, *119*, 1141−1142.

(7) Takada, K.; Diaz, D. J.; Abruña, H. D.; Cuadrado, I.; Casado, C.; Alonso, B.; Moran, M.; Losada, J. *J. Am. Chem. Soc.* **1997**, *119*, 10763−10773. (b) Fillaut, J. L.; Linares, J.; Astruc, D. *Angew. Chem., Int. Ed. Engl.* **1995**, *33*, 2460−2462. (c) Liao, Y. H.; Moss, J. R. *Organomet.* **1995**, *14*, 2130−2132.

(8) Stewart, G. M.; Fox, M. A. *J. Am. Chem. Soc.* **1996**, *118*, 4354−4360. (b) Devadoss, C.; Bharathi, P.; Moore, J. S. *J. Am. Chem. Soc.* **1996**, *118*, 9635−9644.

(9) Hong, B.; Thoms, T. P. S.; Murfee, H. J.; Lebrun, M. J. *Inorg. Chem.* **1997**, *36*, 6146- 6147. (b) Murfee, H. J.; Hong, B. *Polym. Prepr.* **1999**, *40*, 412−413. (c) Murfee, H. J.; Hong, B. *Polym. Prepr.* **2000**, *41*, 431−432.

10.1021/ic000490w CCC: $19.00
Published on Web 10/26/2000

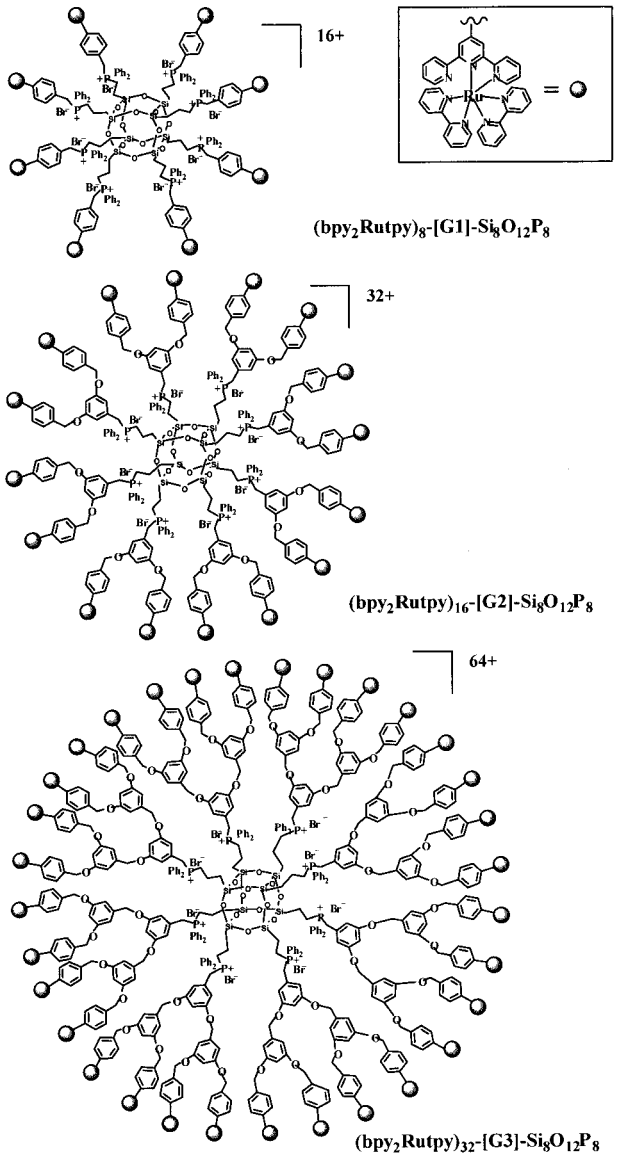

Figure 1. G1−G3 starburst metallodendrimers.

stable core that provides a "starburst" arrangement of eight monodendron arms starting from the first generation. Recently, our group,[9] Feher,[10] and Morris[11] have reported the synthesis of surface-functionalized organic dendrimers with silsesquioxane cores. Our system features an external surface of terpyridine units, which can be readily converted to photoactive and redox-active organometallic moieties by complexation with appropriate transition metals.

We report here the synthesis of terpyridine-functionalized polyether monodendrons, surface-modified organic dendrimers, and the corresponding metallodendrimers with Ru(II)-based chromophores. Specifically, three generations of metallodendrimers, $\{((bpy)_2Ru(tpy))_8\text{-}[G1]\text{-}Si_8O_{12}P_8\}[PF_6]_{16}$, $\{((bpy)_2Ru(tpy))_{16}\text{-}[G2]\text{-}Si_8O_{12}P_8\}[PF_6]_{32}$, and $\{((bpy)_2Ru(tpy))_{32}\text{-}[G3]\text{-}Si_8O_{12}P_8\}[PF_6]_{64}$, have been synthesized and characterized (bpy = 2,2'-bipyridine; tpy = 2,2':6',2''-terpyridine). The external surface features 8, 16, and 32 redox-active and photoactive $(bpy)_2Ru^{II}(tpy)$ units in the G1, G2, and G3 metallodendrimers, respectively. These systems exhibit interesting photophysical and electrochemical properties, including enhanced extinction coefficients, improved overall quantum yields, long-lived excited-state lifetimes, simultaneous redox processes for all metal centers on dendrimer surface, and electrodeposition of films.

Experimental Section

Materials. The monodendrons $(tpy)_1$-[G1]-CH_3 and $(tpy)_1$-[G1]-Br were prepared according to literature methods.[12a] Commercial grade solvents $CHCl_3$, CH_2Cl_2, and diethyl ether were dried over 4 Å molecular sieves prior to use. Tetrahydrofuran (THF) and benzene were dried and deoxygenated by heating to reflux under N_2 for at least 24 h over sodium benzophenone ketyl and were freshly distilled prior to use. Acetone was dried over 4 Å molecular sieves and distilled over K_2CO_3 prior to use. Metallodendrimer samples were purified by column chromatography on basic alumina (Brockman activity I, 60−325 mesh, Fisher Scientific) with acetonitrile as the eluent.

Instrumentation. ^1H, ^{13}C, ^{29}Si, and $^{31}P\{^1H\}$ nuclear magnetic resonance (NMR) spectra were recorded on an Omega 500 MHz spectrometer. Fast atom bombardment mass spectral analysis (FAB/MS) data were obtained on a Micromass (Altrincham, U.K.) Autospec mass spectrometer. Cesium ions at 25 kV were the bombarding species, and the matrix was *meta*-nitrobenzyl alcohol (mNBA). Electrospray mass spectra (ESI/MS) were obtained on a Finnigan LCQ API mass spectrophotometer at Finnigan Corp. Matrix-assisted laser desorption ionization time-of-flight mass spectroscopy (MALDI-TOF/MS) was performed on a PerSeptive Biosystems Voyager-DE Biospectrometry Workstation equipped with a nitrogen laser (emission at 337 nm, 3 ns bursts) and a linear detector. Dithranol (1,8,9-anthracenetriol) was used as the matrix for MALDI-TOF/MS analyses. For each MALDI-TOF/MS measurement, the sample was first dissolved in a suitable solvent and applied to the sample plate, and then dithranol was dissolved and applied over the dried sample spot.

Electrochemical analysis was performed on a CH Instrument 610 electrochemical analyzer, with a platinum disk (1.0 mm diameter) working electrode, a platinum wire counter electrode, and a Ag/AgCl reference electrode. Tetrabutylammonium hexafluorophosphate (Bu_4NPF_6) was used as the electrolyte.

Electronic absorption spectra were recorded on a Hewlett-Packard 8453 UV−visible spectrometer. Steady-state luminescence spectra and quantum yield data were obtained on an Aminco-Bowman Series 2 emission spectrometer. The observed quantum yields of all complexes were measured in spectrograde acetonitrile relative to $Ru(bpy)_3(PF_6)_2$ ($\Phi = 0.062$[12b−c] in acetonitrile) after three freeze−pump−thaw cycles. Time-resolved emission spectroscopy was performed on a nanosecond laser flash photolysis unit equipped with a Continuum Surelite II-10 Q-switched Nd:YAG laser and Surelite OPO (optical parametric oscillator) tunable visible source, a LeCroy 9350A oscilloscope, and a Spex 270 MIT-2x-FIX high-performance scanning and imaging spectrometer. The resulting signals were fitted as single exponential, resulting in the best fit with respect to both the recorded phase and intensity information.

$(tpy)_2$-[G2]-OH. 3,5-Dihydroxybenxyl alcohol (184 mg, 1.32 mmol), potassium carbonate (472 mg, 3.42 mmol), 18-crown-6 (139 mg, 0.525 mmol), and $(tpy)_1$-[G1]-Br (1.145 g, 2.85 mmol) were placed in a 100 mL three-neck round-bottom flask, which was purged and degassed with nitrogen. Freshly distilled acetone (175 mL) was added via syringe, and the solution was refluxed for 48 h. Acetone was then removed under reduced pressure, and the compound was dissolved in chloroform and washed with brine. The separated chloroform solution then was dried over anhydrous sodium sulfate for ca. 4 h. It was then reduced to minimal volume under reduced pressure and added dropwise to a vigorously stirred diethyl ether solution. A white precipitate was collected on a glass frit, washed with clean diethyl ether, and dried in vacuo overnight. Yield: 743 mg, 72%. ^1H NMR ($CDCl_3$): δ 8.70 (s, 8H), 8.63 (d, 4H), 7.86 (m, 8H), 7.52 (d, 4H), 7.33 (m, 4H), 6.64 (s,

(10) Feher, F. J.; Wyndham, K. D. *Chem. Commun.* **1998**, 323−324.
(11) Coupar, P. I.; Jaffrés, P. A.; Morris, R. E. *J. Chem. Soc., Dalton Trans.* **1999**, 2183−2187. (b) Jaffrés, P. A.; Morris, R. E. *J. Chem. Soc., Dalton Trans.* **1998**, 2767−2770.
(12) Collin, J. P.; Guillerez, S.; Sauvage, J. P.; Barigelletti, F.; De Cola, L.; Flamigni, L.; Balzani, V. *Inorg. Chem.* **1991**, *30*, 4230−4238. (b) Caspar, J. V.; Meyer, T. J. *J. Am. Chem. Soc.* **1983**, *105*, 5583. (c) Caspar, J. V.; Sullivan, B. P.; Meyer, T. J. *Inorg. Chem.* **1984**, *23*, 2104.

2H), 6.55 (s, 1H), 5.07 (s, 4H), 4.65 (s, 2H) ppm. ^{13}C NMR ($CDCl_3$): δ 159.97, 156.13, 155.83, 149.77, 137.94, 136.91, 132.09, 128.55, 127.88, 127.46, 123.82, 121.41, 118.80, 105.86, 101.27, 69.59 (Ph*C*H_2-OPh), 65.11 (*C*H_2OH) ppm. FAB/MS: *m*/*z* 783, $[M]^+$. MALDI-TOF/MS: *m*/*z* 783.5, $[M]^+$.

(tpy)$_2$-[G2]-Br. (tpy)$_2$-[G2]-OH (701 mg, 0.895 mmol) was placed in a 100 mL three-neck round-bottom flask, which was purged and degassed with nitrogen. Distilled THF (40 mL) was added under a strong nitrogen flow, and then carbon tetrabromide (891 mg, 2.69 mmol) and triphenylphosphine (703 mg, 2.68 mmol) were added. The solution was stirred at room temperature for 2 h, and 100 mL of DI H_2O was added. Tetrahydrofuran was removed under reduced pressure. Chloroform was added, and this solution was washed with distilled water. The separated chloroform solution was dried over anhydrous sodium sulfate for ca. 4 h. This chloroform solution was then reduced to a minimal volume under reduced pressure and added dropwise to a vigorously stirred diethyl ether solution. An off-white precipitate was collected on a glass frit, washed with diethyl ether, and dried in vacuo overnight. Yield: 486 mg, 64%. ^{1}H NMR ($CDCl_3$): δ 8.71 (s, 8H), 8.63 (m, 4H), 7.89 (m, 4H), 7.54 (d, 4H), 7.34 (ddd, 4H), 5.11 (s, 4H), 4.44 (s, 2H) ppm. ^{13}C NMR ($CDCl_3$): δ 159.97, 155.86, 155.23, 149.77, 149.08, 143.72, 137.94, 127.56, 123.87, 127.46, 123.82, 121.41, 118.82, 108.33, 102.13, 69.73 (Ph*C*H_2OPh), 29.72 (*C*H_2Br) ppm. FAB/MS: *m*/*z* 847, $[M + H]^+$. MALDI-TOF/MS: *m*/*z* 847.4, $[M + H]^+$.

(tpy)$_4$-[G3]-OH. 3,5-Dihydroxybenxyl alcohol (44 mg, 0.314 mmol), potassium carbonate (91.2 mg, 0.659 mmol), 18-crown-6 (80.6 mg, 0.305 mmol), and (tpy)$_1$-[G1]-Br (509 g, 0.601 mmol) were placed in a 100 mL three-neck round-bottom flask, which was purged and degassed with nitrogen. THF (25 mL) and benzene (25 mL) were added via syringe, and the solution was refluxed for 48 h. The reaction was brought to dryness under reduced pressure, and the resulting solid was dissolved in chloroform and washed with brine. The separated chloroform solution was then dried over anhydrous sodium sulfate for ca. 4 h. It was then reduced to minimal volume under reduced pressure, and a white precipitate was isolated out of diethyl ether. This was collected on a glass frit, washed with clean diethyl ether, and dried in vacuo overnight. Yield: 301 mg, 58%. ^{1}H NMR ($CDCl_3$): δ 8.70 (s, 16H), 8.64 (m, 8H), 7.86 (m, 8H), 7.50 (d, 8H), 7.32 (ddd, 4H), 5.05 (s, 8H), 4.95 (s, 4H), 4.64 (s, 2H) ppm. ^{13}C NMR ($CDCl_3$): δ 159.77, 156.01, 155.95, 155.67, 155.46, 149.59, 148.89, 137.65, 136.91, 136.67, 135.60, 127.75, 127.26, 127.11, 125.33, 123.75, 123.62, 121.39, 121.19, 118.60, 70.30, 69.45 (Ph*C*H_2OPh), 64.69 (*C*H_2OH) ppm. FAB/MS: *m*/*z* 1670, $[M]^+$. MALDI-TOF/MS: *m*/*z* 1671.0, $[M + H]^+$.

(tpy)$_4$-[G3]-Br. In a reaction similar to the synthesis of (tpy)$_2$-[G2]-Br, (tpy)$_4$-[G3]-OH (297 mg, 0.178 mmol), carbon tetrabromide (187 mg, 0.563 mmol), and triphenylphosphine (152 mg, 0.579) were used. Yield: 170 mg, 60%. ^{1}H NMR ($CDCl_3$): δ 8.74−7.30 (m, 56H), 6.69−6.55 (m, 6H), 5.10 (s, 8H), 4.99 (s, 4H), 4.43 (s, 2H) ppm. ^{13}C NMR ($CDCl_3$): δ 159.90, 156.02, 155.74, 148.94, 137.92, 137.70, 127.80, 127.32, 127.21, 123.64, 121.15, 118.67, 118.62, 106.27, 101.66, 69.82, 69.57 (Ph*C*H_2OPh), 33.53 (*C*H_2Br) ppm. FAB/MS: *m*/*z* 1734, $[M + H]^+$. MALDI-TOF/MS: *m*/*z* 1733.6, $[M + H]^+$.

(tpy)$_8$-[G1]-Si$_8$O$_{12}$P$_8$. (tpy)$_1$-[G1]-Br (569 mg, 1.414 mmol) and [G0]-$Si_8O_{12}P_8$ (300 mg, 0.141 mmol) were placed into a 100 mL three-neck round-bottom flask, which was then removed from the drybox and attached to a Schlenk line. THF (125 mL) was added via syringe, and the solution was refluxed for 24 h. Cooling to room temperature afforded a white precipitate, which was collected on a swivel frit (Schlenk filter). The solid was washed with diethyl ether under N_2, and the reaction apparatus was brought back into the drybox for sample collection. The sample is soluble in $CHCl_3$, CH_2Cl_2, and hot THF. Yield: 457 mg, 61%. ^{1}H NMR ($CDCl_3$): δ 8.61−7.08 (m, Ar-*H*, 192H), 5.30 (m, PhC*H*$_2$P, 16H), 3.75 (m, PC*H*$_2$CH$_2$Si, 16H), 1.85 (m, PCH$_2$C*H*$_2$Si, 16H) ppm. ^{13}C NMR ($CDCl_3$): δ 155.49, 149.40, 148.99, 137.14, 134.90, 134.84, 134.72, 130.07, 127.50, 124.32, 124.46, 121.27, 118.99, 105.34, 65.99 (P*C*H$_2$Ph), 57.50 (P*C*H$_2$CH$_2$Si), 15.42 (PCH$_2$*C*H$_2$-Si) ppm. ^{31}P{^{1}H} NMR ($CDCl_3$): δ 30.99 ppm. ^{29}Si NMR ($CDCl_3$): δ −67.9 ppm.

(tpy)$_{16}$-[G2]-Si$_8$O$_{12}$P$_8$. In a drybox, (tpy)$_2$-[G2]-Br (77 mg, 0.091 mmol) and [G0]-$Si_8O_{12}P_8$ (21.4 mg, 0.01 mmol) were placed into a 100 mL three neck round-bottom flask, which was then removed from the drybox and attached to a Schlenk line. THF (30 mL, distilled) was added via syringe, and the resulting solution was refluxed for 48 h. The solution was concentrated under reduced pressure, and the resulting mixture was added dropwise to a stirring diethyl ether solution to afford a white precipitate. The solid was washed with diethyl ether under N_2, and the reaction apparatus was brought back into the drybox. The sample is soluble in THF, $CHCl_3$, and CH_2Cl_2. Yield: 56.3 mg, 63%. ^{1}H NMR ($CDCl_3$): δ 8.79−7.26 (m, Ar-*H*), 6.70−6.61 (m, Ar-*H*), 5.15 (tpy-Ph-C*H*$_2$O), 4.45 (PhC*H*$_2$P, 16H), 3.76 (m, PC*H*$_2$CH$_2$Si, 16H), 1.85 (m, PCH$_2$C*H*$_2$Si, 16H) ppm. ^{13}C NMR ($CDCl_3$): δ 155.71, 155.59, 155.52, 155.47, 148.84, 148.77, 136.83, 136.78, 134.46, 134.38, 134.29, 130.29, 127.19, 123.75, 121.29, 118.59, 105.01, 69.22 (Ph*C*H$_2$O), 67.82 (P*C*H$_2$Ph), 50.38 (P*C*H$_2$CH$_2$Si), 25.25 (PCH$_2$*C*H$_2$Si) ppm. ^{31}P{^{1}H} NMR ($CDCl_3$): δ 31.80 ppm. ^{29}Si NMR ($CDCl_3$): δ −69.0 ppm.

(tpy)$_{32}$-[G3]-Si$_8$O$_{12}$P$_8$. In a procedure similar to that of (tpy)$_{16}$-[G2]-$Si_8O_{12}P_8$, the compounds (tpy)$_4$-[G3]-Br (117.4 mg, 0.068 mmol) and [G0]-$Si_8O_{12}P_8$ (14.5 mg, 0.0068 mmol) were reacted. A 50 mL volume of distilled THF was used, and the solution was heated to reflux for 72 h. The sample is soluble in THF, $CHCl_3$, and CH_2Cl_2. Yield: 92 mg, 85%. ^{1}H NMR ($CDCl_3$): δ 8.91−7.21 (m, Ar-*H*), 6.70−6.56 (m, Ar-*H*), 5.11 (tpy-Ph-C*H*$_2$O), 4.99 (Ph-C*H*$_2$O, 32H), 4.53 (PhC*H*$_2$P, 16H), 3.75 (m, PC*H*$_2$CH$_2$Si, 16H), 1.85 (m, PCH$_2$C*H*$_2$Si, 16H) ppm. ^{13}C NMR ($CDCl_3$): δ 160.01, 155.91, 155.66, 149.88, 149.76, 148.90, 137.90, 137.76, 137.14, 136.99, 127.90, 127.65, 127.48, 127.42, 127.30, 123.82, 121.56, 121.39, 118.84, 117.98, 116.80, 107.79, 106.37, 102.05, 101.73, 69.92 (tpy-Ph-*C*H$_2$O), 69.78 (Ph*C*H$_2$O), 69.64 (P*C*H$_2$Ph), 46.30 (P*C*H$_2$-CH$_2$Si), 29.50 (PCH$_2$*C*H$_2$Si) ppm. ^{31}P{^{1}H} NMR ($CDCl_3$): δ 35.22 ppm.

Metallodendrimer Synthesis. In general, ca. 8, 16, or 32 equiv of $(bpy)_2RuCl_2\cdot 2H_2O$ was reacted with 1 equiv of (tpy)$_8$-[G1]-$Si_8O_{12}P_8$, (tpy)$_{16}$-[G2]-$Si_8O_{12}P_8$, or (tpy)$_{32}$-[G3]-$Si_8O_{12}P_8$, respectively. Both starting materials were placed into a 100 mL three-neck round-bottom flask, which was purged and degassed with nitrogen. Distilled THF (40 mL) and degassed ethylene glycol (10 mL) were added, and the solution was refluxed for ca. 96 h. The solution was cooled, and excess NH_4PF_6 was added. THF was then removed under reduced pressure, and the resulting ethylene glycol solution was heated to 120−130 °C for ca. 4 h. This was again cooled to room temperature and transferred to an aqueous saturated solution of KPF_6 to give the product, which was collected by vacuum filtration, washed with diethyl ether, and dried in vacuo overnight. The samples were then purified by column chromatography (basic alumina, Brockman activity I, 60−325 mesh) with acetonitrile as eluent. For each metallodendrimer sample, two fractions were recovered. The first fraction was determined to be the unreacted starting materials and was discarded. The second fraction was condensed under reduced pressure, precipitated out of diethyl ether, collected on a glass frit, and dried in vacuo overnight. Amounts of reagents used for each metallodendrimer and yields after column chromatographic purification are as follows: for the G1 metallodendrimer, (tpy)$_8$-[G1]-$Si_8O_{12}P_8$ (98.5 mg, 0.0184 mmol) and $(bpy)_2RuCl_2\cdot 2H_2O$ (80.0 mg, 0.1537 mmol) were used. Yield: 90.5 mg, 45%. ^{31}P{^{1}H} NMR (CD_3CN): δ 31.46 ppm. For the G2 metallodendrimer, (tpy)$_{16}$-[G2]-$Si_8O_{12}P_8$ (100.0 mg, 0.0112 mmol) and $(bpy)_2RuCl_2\cdot 2H_2O$ (100.5 mg, 0.193 mmol) were used. Yield: 49.1 mg, 22%. ^{31}P{^{1}H} NMR (CD_3CN): δ 31.05 ppm. For the G3 metallodendrimer, (tpy)$_{32}$-[G3]-$Si_8O_{12}P_8$ (28.0 mg, 0.0018 mmol) and $(bpy)_2RuCl_2\cdot 2H_2O$ (37.1 mg, 0.0713 mmol) were used. Yield: 29.9 mg, 45%. ^{31}P{^{1}H} NMR (CD_3CN): δ 29.41 ppm.

{(bpy)$_2$Ru(tpy)$_1$-[G1]-CH$_3$}[PF$_6$]$_2$. In a process similar to the metallodendrimer synthesis, the compounds (tpy)$_1$-[G1]-CH_3 (36.6 mg, 0.113 mmol) and $(bpy)_2RuCl_2\cdot 2H_2O$ (49.7 mg, 0.0955 mmol) were used. The product of this reaction was also processed and purified in the same manner as the metallodendrimers. Yield after column chromatographic purification: 19.1 mg, 20%. ^{1}H NMR (CD_3CN): δ 6.45−8.80 (Ar-*H*), 2.42 (−C*H*$_3$). ESI/MS: *m*/*z* 882.33, $[M - PF_6]^+$.

Results and Discussion

Synthesis and Characterization of Monodendrons. A convergent synthesis was used to prepare monodendrons with terminal terpyridyl groups, Figure 2. Such a synthesis was initiated at the periphery and propagated to the focal point of

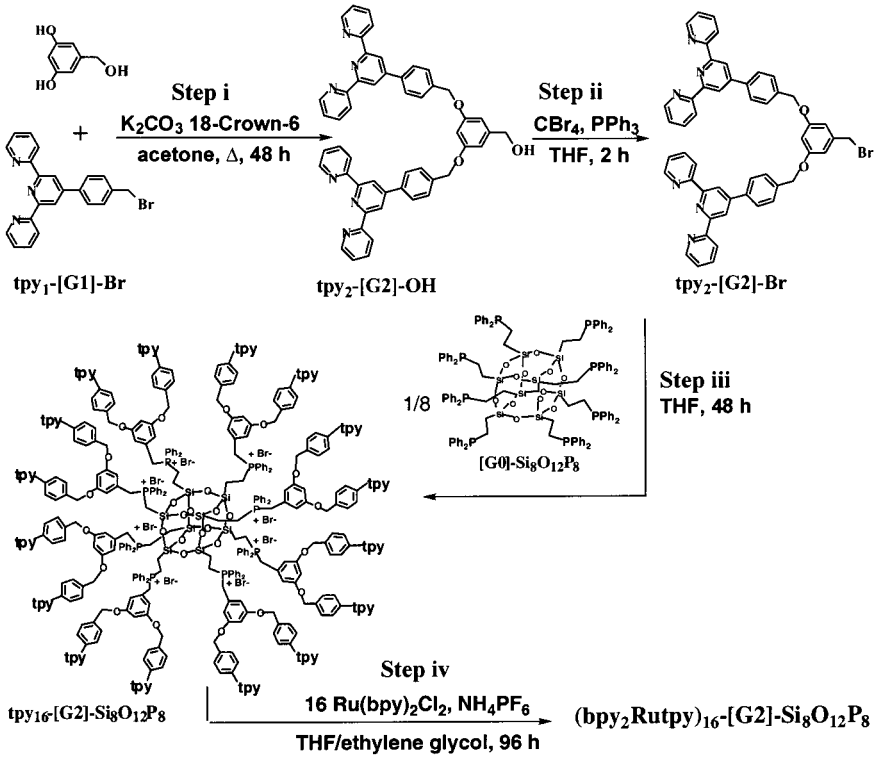

Figure 2. Representative synthesis of G2 monodedrons and dendrimers.

Table 1. NMR (^{1}H and ^{13}C) and Mass Spectral (FAB and MALDI-TOF) Data

compd	^{1}H NMR (ppm)	^{13}C NMR (ppm)	FAB/MS (*m*/*z*)	MALDI-TOF/MS (*m*/*z*)
$(tpy)_1$-[G_1]-Br	4.43 ($-CH_2$Br)	33.01 ($-CH_2$Br)	402, $[M - H]^+$	403.9, $[M + H]^+$
$(tpy)_2$-[G_2]-OH	4.65 ($-CH_2$OH)	65.11 ($-CH_2$OH)	783, $[M]^+$	783.5, $[M]^+$
$(tpy)_2$-[G_2]-Br	4.44 ($-CH_2$Br)	29.72 ($-CH_2$Br)	847, $[M + H]^+$	847.4, $[M]^+$
$(tpy)_4$-[G_3]-OH	4.64 ($-CH_2$OH)	64.69 ($-CH_2$OH)	1670, $[M]^+$	1671.0, $[M + H]^+$
$(tpy)_4$-[G_3]-Br	4.43 ($-CH_2$Br)	33.53 ($-CH_2$Br)	1734, $[M + H]^+$	1733.6, $[M + H]^+$

the dendrimer.[1e−g,2] Treatment of $(tpy)_1$-[G1]-Br[12a] (2 equiv) with 3,5-dihydroxybenzyl alcohol (step i) afforded the second generation monodendron $(tpy)_2$-[G2]-OH.[2d,9] Further bromination with CBr_4/PPh_3 (step ii) yielded $(tpy)_2$-[G2]-Br. By repetition of steps i and ii, $(tpy)_4$-[G3]-OH and $(tpy)_4$-[G3]-Br can be prepared from $(tpy)_2$-[G2]-Br.

All monodendrons were fully characterized using ^{1}H and ^{13}C NMR, as well as FAB and MALDI-TOF mass spectral analysis. Upon conversion from the benzylic alcohol to benzylic bromide, the ^{1}H NMR signal of the focal point $-CH_2$ units shifted from ca. 4.65 ppm in the former to ca. 4.44 ppm in the latter. Correspondingly, the ^{13}C NMR signal of the benzylic $-CH_2$ group also changed from ca. 65 ppm for the alcohol to 29−33 ppm for the brominated species. In addition, FAB/MS and MALDI-TOF/MS offered clear identification of the molecular ion peaks in the form of M^+, $[M - H]^+$, or $[M + H]^+$ for all monodendrons, Table 1.

Synthesis of Organic Dendrimers. G1−G3 dendrimers were prepared by attaching terpyridine-functionalized monodendrons around the periphery of an octafunctionalized silsesquioxane, $Si_8O_{12}(CH_2CH_2PPh_2)_8$ ([G0]-$Si_8O_{12}P_8$), Figure 2. Direct coupling reactions between the terminal $-PPh_2$ units of the silsesquioxane with the focal point −Br units of monodendrons provided phosphonium groups at the points of attachment. A noteworthy feature of this synthesis is that $^{31}P\{^1H\}$ NMR can be used to monitor the completion of the reaction and confirm the purity of the organic dendrimer products after purification using column chromatography. Typically, the synthesis of dendrimers $(tpy)_m$-[G*n*]-$Si_8O_{12}P_8$ ($n = 1$, $m = 8$; $n = 2$, $m = 16$; $n = 3$, $m = 32$) consisted of reacting ca. 8 equiv of the monodendrons $(tpy)_m$-[G*n*]-Br ($n = 1$, $m = 1$; $n = 2$, $m = 2$; $n = 3$, $m = 4$) with 1 equiv of the silsesquioxane [G0]-$Si_8O_{12}P_8$ in refluxing THF (step iii, Figure 2). The resulting G1−G3 dendrimers are slightly air sensitive and must be stored under an inert atmosphere to prevent the slow decomposition.

Characterization of Organic Dendrimers. Evidence for the complete transformation from eight terminal phosphines in [G0]-$Si_8O_{12}P_8$ to the eight phosphonium linkage units was provided by the complete disappearance of the $^{31}P\{^1H\}$ NMR signal of free $-PPh_2$ at −9.37 ppm and the appearance of the phosphonium $^{31}P\{^1H\}$ NMR signal in the region of 30−36 ppm for $(tpy)_m$-[G*n*]-$Si_8O_{12}P_8$. Specifically, the $^{31}P\{^1H\}$ NMR chemical shifts of the G1−G3 dendrimers are 30.99, 31.80, and 35.22 ppm, respectively. Solution-state ^{29}Si NMR spectroscopy was also performed, with signals at −67.8 and −68.9 ppm for the G1 and G2 dendrimers, respectively. Though shifted, these signals are in the region expected for a silsesquioxane structure.[9,10] No significant ^{29}Si NMR peak was observed for the G3 dendrimer, presumably due to the increased molecular weight and the reduced percentage of ^{29}Si nuclei available in this macromolecule.

Mass spectral analyses of these dendrimers are accomplished using ESI/MS and MALDI-TOF/MS. FAB/MS failed to provide satisfactory results due to the relatively high molecular weight of even the first generation dendrimer (MW = 5341 Da). Instead, ESI/MS analysis of G1 dendrimer provided a simple mass pattern and allowed the accurate determination of molecular mass with high sensitivity. Figure 3 is a representative

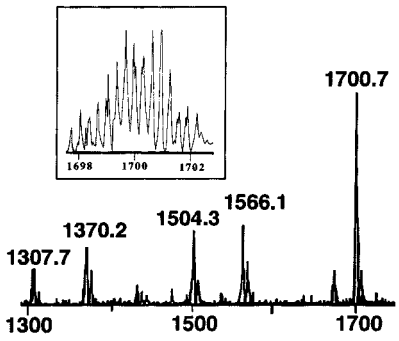

Figure 3. ESI/MS of the G1 dendrimer, $(tpy)_8$-[G1]-$Si_8O_{12}P_8$.

Table 2. ESI/MS Analysis of $(tpy)_8$-[G1]-$Si_8O_{12}P_8$ (M)

obsd *m*/*z*[a]	calcd *m*/*z*	peak assgnt
1700.7	1700.3	$[M - 3Br]^{3+}$
1566.1	1566.3	$[M - 3Br - (tpy)_1\text{-}[G1]Br]^{3+}$
1504.3	1504.6	$[M - 3Br - (tpy)_1\text{-}[G1]\text{-}Br - PPh_2]^{3+}$
1370.2	1370.5	$[M - 3Br - 2(tpy)_1\text{-}[G1]\text{-}Br - PPh_2]^{3+}$
1307.7	1308.8	$[M - 3Br - 2(tpy)_1\text{-}[G1]\text{-}Br - 2PPh_2]^{3+}$

[a] Relative abundances of all other fragments of the full ESI/MS spectrum, in addition to those listed here, are <10%.

spectrum of $(tpy)_8$-[G1]-$Si_8O_{12}P_8$ with inset of the peak at *m*/*z* 1700.7 (isotope peaks separated by 0.3 *m*/*z* units). Interestingly, the spectrum is dominated by five sets of peaks, all with $z = 3$. The assignment of peaks is relatively straightforward, as listed in Table 2. Consecutive loss of $(tpy)_1$-[G1]-Br and PPh_2 units is observed. From both ESI/MS and $^{31}P\{^1H\}$ NMR analyses we conclude that the deposition of eight monodendron arms on the octafunctionalized silsesquioxane core is essentially complete, and no significant imperfection of the dendrimer is observed. However, further efforts to obtain the ESI/MS spectra for the G2 and G3 dendrimers were unsuccessful.

The successful characterization of all generations of organic dendrimers was only achieved using MALDI-TOF/MS analysis. The peak assignments, along with the observed and calculated *m*/*z* values, are listed in Table 3. Several unique and interesting features were observed in the fragmentation pattern of these dendrimers:

(i) In general, a clear pattern of consecutive loss of Br^- counteranions and G1 ($m/z = 323$), G2 ($m/z = 766$), or G3 ($m/z = 1653$) monodendrons (without focal point Br) was observed. Figure 4 shows a representative MALDI-TOF/MS mass spectrum for the G2 dendrimer, $(tpy)_{16}$-[G2]-$Si_8O_{12}P_8$, where the consecutive losses of G2 monodendron and Br^- are observed. The peak assignments of MALDI-TOF/MS data of metallodendrimers are listed in Table 3. The aforementioned $^{31}P\{^1H\}$ NMR analysis showed that each of these dendrimers displayed a single peak, with no additional peaks corresponding to the free $-PPh_2$ units. Hence, both MALDI-TOF/MS and $^{31}P\{^1H\}$ NMR data suggest a complete conversion from the silsesquioxane starting material to the corresponding dendrimer, and the observed fragmentation takes place during the MALDI-TOF/MS analysis. A similar pattern was also observed in the aforementioned ESI/MS analysis of $(tpy)_8$-[G1]-$Si_8O_{12}P_8$. Previously, the presence of dimeric or trimeric species was reported for neutral dendrimers such as phenylacetylene and aromatic polyether dendrimers.[13] However, no significant peaks corresponding to the dimers or trimers of our dendrimers have been observed here.

(ii) Although no K^+ or Li^+ salts were added to the samples, the dithranol matrix afforded peaks with the addition of K^+ and Li^+, especially in the spectra of the G1 and G3 dendrimers (Table 3). Observations of such peaks are not unusual in the MALDI-TOF/MS analysis of polymers and neutral dendrimers.[13b−d,14] These peaks were attributed to the strong complexing properties of large oligomers or fragments with alkali metal cations.

(iii) The addition of O atoms upon fragmentation was also observed. Previously, we have observed similar characteristics in the FAB/MS analysis of low-dimensional molecular rods with rigid polyphosphine spacers such as $(Ph_2P)_2C{=}(C)_n{=}C(PPh_2)_2$ ($n = 1, 2$).[15] The additions of one or multiple O atoms to the molecular ion or oligomeric fragments of the spacers and their metal complexes were observed in those systems. Here, the similar observation in metallodendrimers can also be ascribed to the phosphine oxidation during the ionization process of MALDI-TOF/MS. Upon loss of the Br− counteranions and monodendrons in the MALDI-TOF/MS analysis of the dendrimers, the bare PPh_2 units in the molecular fragments can be oxidized and give peaks with extra O atoms.

Synthesis and Characterization of Metallodendrimers. Complexation of the G1−G3 dendrimers with the Ru(II) starting material was achieved by a straightforward synthetic procedure, Figure 2. Preparation of G1−G3 metallodendrimers was accomplished by reacting the corresponding tpy-terminated dendrimers $(tpy)_m$-[G*n*]-$Si_8O_{12}P_8$ with ca. 8, 16, or 32 equiv of $(bpy)_2RuCl_2{\cdot}2H_2O$, respectively. Upon synthesis, each metallodendrimer was purified using column chromatographic separation with basic alumina and acetonitrile eluent. The desired product was collected as the second fraction. The samples thus obtained were characterized and studied by a variety of methods, including $^{31}P\{^1H\}$ NMR, electronic absorption, steady-state and time-resolved emission, quantum yield measurements, and electrochemical analysis. Specifically, $^{31}P\{^1H\}$ NMR chemical shifts of 31.46, 31.05, and 29.41 ppm were observed for G1, G2, and G3, respectively. These values, though slightly different, match the data of the corresponding nonmetalated dendrimers. All metallodendrimers are soluble in acetonitrile.

Elemental analysis (EA) was attempted for the metallodendrimers; however, the experimental results were lower than the calculated values. Although all complexes were purified by column chromatographic separations, however, due to surface bulk, trapped solvent molecules have been known to cause lower than expected percent carbon, nitrogen, and hydrogen.[3b,3g−h] Repeated attempts at removing trapped solvent by high vacuum pumping and reprecipitation out of diethyl ether proved unsuccessful in obtaining satisfactory EA data. Unsatisfactory results were also encountered during the elemental analysis of metallodendrimers containing Au(II) and Ru(II) centers.[3b,g]

To facilitate the electrochemical and photophysical analyses of the metallodendrimers, a monomeric model compound, $\{(bpy)_2Ru(tpy)_1\text{-}[G1]\text{-}CH_3\}[PF_6]_2$, was prepared. A discussion of the photophysical and electrochemical characteristics of these compounds is given below.

(13) Xu, Z. F.; Kahr, M.; Walker, K. L.; Wilkins, C. L.; Moore, J. S. *J. Am. Chem. Soc.* **1994**, *116*, 4537−4550. (b) Leon, J. W.; Fréchet, J. M. J. *Polym. Bull.* **1995**, *35*, 449−455. (c) Vitalini, D.; Mineo, P.; Dibella, S.; Fragala, I.; Maravigna, P.; Scamporrino, E. *Macromolecules* **1996**, *29*, 4478−4485. (d) Juhasz, P.; Costello, C. E. *Rapid Commun. Mass Spectrom.* **1993**, *7*, 343−351.

(14) Montaudo, G.; Montaudo, M. S.; Puglisi, C.; Samperi, F.; Sepulchre, M. *Macromol.Chem. Phys.* **1996**, *197*, 2615−2625. (b) Montaudo, G.; Montaudo, M. S.; Puglisi, C.; Samperi, F. *Rapid Commun. Mass Spectrom.* **1995**, *9*, 453−460. (c) Burger, H. M.; Muller, H. M.; Seebach, D.; Bornsen, K. O.; Schar, M.; Widmer, H. M. *Macromolecules* **1993**, *26*, 4783−4790.

(15) Hong, B.; Ortega, J. V. *Angew. Chem., Int. Ed. Engl.* **1998**, *37*, 2131−2134. (b) Hong, B.; Woodcock, S. R.; Saito, S. K.; Ortega, J. V. *J. Chem. Soc., Dalton Trans.* **1998**, 2615−2623.

Table 3. MALDI-TOF/MS Data for Dendrimers

compd	obsd (*m*/*z*)	calcd (*m*/*z*)	peak assgnt[a]
$(tpy)_8$-[G1]-$Si_8O_{12}P_8$	5266	5267	$[M - 1Br + Li]^+$
	5248	5252	$[M - 2Br + K + 2O]^+$
	5187	5188	$[M - 2Br + Li]^+$
	5169	5172	$[M - 3Br + K + 2O]^+$
	5108	5108	$[M - 3Br + Li]^+$
	5099	5099	$[M - 4Br + 2K]^+$
	4864	4866	$[M - 2Br - 1G1\ dendron + Li]^+$
	4847	4849	$[M - 3Br - 1G1\ dendron + K + 2O]^+$
	4773	4774	$[M - 2G1\ dendron + 2K]^+$
	4445	4445	$[M - 3G1\ dendron + K + 2O]^+$
	4372	4373	$[M - 3G1\ dendron]^+$
$(tpy)_{16}$-[G2]-$Si_8O_{12}P_8$	8808	8809	$[M - 1Br]^+$
	7961	7963	$[M - 2Br - 1G2\ dendron]^+$
	7131	7133	$[M - 3Br - 2G2\ dendron + 1O]^+$
	6301	6303	$[M - 4Br - 3G2\ dendron + 2O]^+$
	5471	5473	$[M - 5Br - 4G2\ dendron + 3O]^+$
	4657	4659	$[M - 5Br - 5G2\ dendron]^+$
	3767	3766	$[M - 7Br - 6G2\ dendron]^+$
$(tpy)_{32}$-[G3]-$Si_8O_{12}P_8$	15196	15194	$[M - 1Br - 1G2\ dendron + K + O]^+$
	14230	14227	$[M - 2Br - 1G3\ dendron + K + O]^+$
	13338	13333	$[M - 3Br - 1G3\ dendron - 1G2\ dendron + Li]^+$
	12552	12558	$[M - 2Br - 2G3\ dendron + K]^+$
	11642	11640	$[M - 4Br - 2G3\ dendron - 1G2\ dendron + 2\ Na]^+$
	9946	9947	$[M - 4Br - 3G3\ dendron - 1G2\ dendron + Li]^+$
	9051	9054	$[M - 4Br - 4G3\ dendron]^+$
	8124	8128	$[M - 6Br - 4G3\ dendron - 1G2\ dendron]^+$

[a] G1 dendron $m/z = 323$, G2 dendron $m/z = 766$, and G3 dendron $m/z = 1653$.

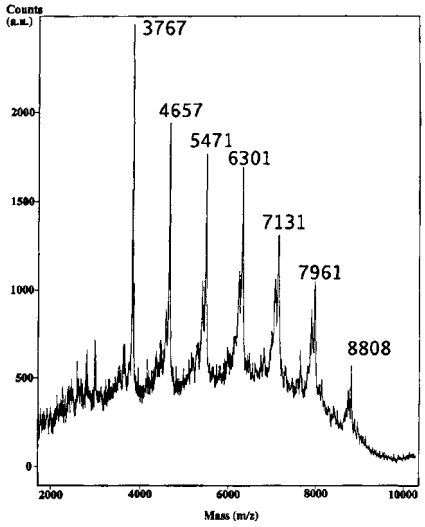

Figure 4. MALDI-TOF/MS spectrum of the G2 dendrimer, $(tpy)_{16}$-[G2]-$Si_8O_{12}P_8$.

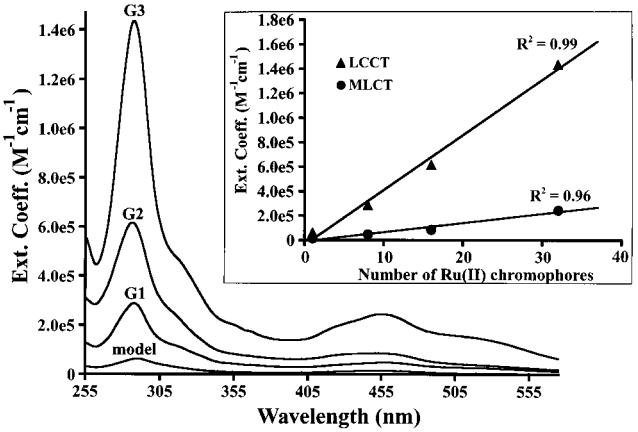

Figure 5. Overlay of UV/vis spectra of the G1−G3 metallodendrimers and monomeric model compound $\{(bpy)_2Ru(tpy)_1$-[G1]-$CH_3\}[PF_6]_2$. Slopes for the inset are 44 895 for the LCCT band and 7485 for the MLCT band, given fitting equation as $y = ax + b$, y being the extinction coefficient and x being the number of chromophores.

Molecular Photophysics. Photophysical analysis of the G1−G3 metallodendrimers consisted of electronic absorption, quantum yield, excited-state lifetime, and steady-state emission analysis. Figure 5 compares the electronic absorption spectra of the G1−G3 metallodendrimers and the model compound. The extinction coefficients for the metallodendrimers (Table 4) are much larger than that of the model compound, which is indicative of a chromophore summation effect.[3a,b] These results show an increase in extinction coefficient that coincides with the number of surface-confined Ru(II) metal centers in metallodendrimers, Figure 5. Specifically, the extinction coefficients of the G1−G3 metallodendrimers at 288 nm (ligand-centered charge transfer, LCCT) and 455 nm (metal to ligand charge transfer, MLCT) were increased approximately proportional to the number of surface-confined Ru(II) metal centers, Figure 5. This is significant in that we do not observe a drop-off in the extinction coefficients when changing from lower to higher generations in our complexes. In a previous study, the metallodendrimers with a polyamidoamide (PAMAM) framework and terminal $Ru(bpy)_3^{2+}$ chromophores did not exhibit this near-proportionality in extinction coefficients as the generation number increased, which was attributed to solvent molecules trapped within the dendrimer cavities.[3b] Hence, in addition to the $^{31}P\{^1H\}$ NMR analysis, the electronic absorption data also confirm that we have a statistically significant amount of fully converted metallodendrimers.

All metallodendrimers with terminal Ru(II)-based chromophores were emissive at room temperature. Single exponential decay kinetics were observed, with lifetimes of 805, 605, 890, and 880 ns for the model compound, G1, G2, and G3 metallodendrimers, respectively (excitation at 455 nm and monitoring emission wavelengths in the range of 605−610 nm). A representative decay trace for the G2 metallodendrimer is given in Figure 6. The emission wavelengths were 608−611

Table 4. Photophysical Data for Metallodendrimers

compd	λ_{max} (nm)	ϵ (M^{-1} cm^{-1})	λ_{em} (nm)[b]	lifetime (ns)
$\{((bpy)_2Ru(tpy))_8$-[G1]-$Si_8O_{12}P_8\}[PF_6]_{16}$	245[a]	142 397	611	605
	255[a]	126 046		
	288	287 082		
	314[a]	118 663		
	456	46 764		
	530[a]	23 743		
$\{((bpy)_2Ru(tpy))_{16}$-[G2]-$Si_8O_{12}P_8\}[PF_6]_{32}$	243[a]	336 813	608	890
	252[a]	313 425		
	286	615 478		
	316[a]	239 334		
	453	84 751		
	535[a]	32 199		
$\{((bpy)_2Ru(tpy))_{32}$-[G3]-$Si_8O_{12}P_8\}[PF_6]_{64}$	239[a]	681 980	609	880
	255[a]	558 580		
	288	1 434 391		
	315[a]	481 736		
	455	243 235		
	530[a]	135 893		
$\{(bpy)_2Ru(tpy)_1$-[G1]$CH_3\}[PF6]_2$	246	32 606	605	805
	290	62 278		
	455	14 005		

[a] Shoulder of main peak. [b] 298 K, spectrograde acetonitrile solution, $\lambda_{ex} = 455$ nm.

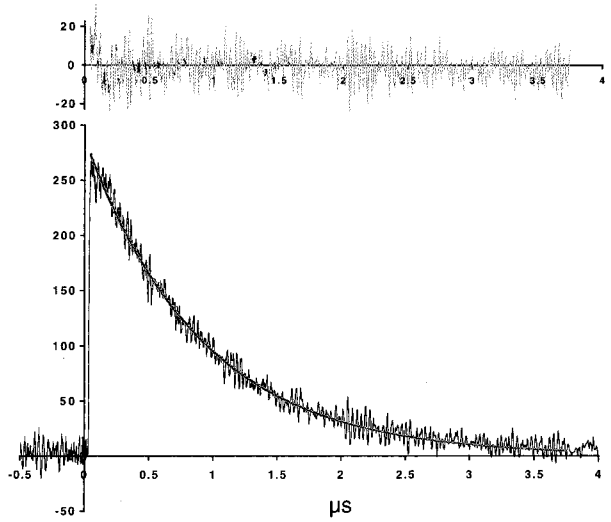

Figure 6. Excited-state decay trace of the G2 metallodendrimer: excitation wavelength 450 nm; spectrograde acetonitrile; 22 °C; monitoring emission wavelength 610 nm.

nm for all three generations upon excitation at 455 nm, Table 4. These data confirm that the surface-confined chromophores are isolated and only one type of emissive excited state is observed, namely, the ^{3}MLCT state of terminal $(-CH_2$-Ph-tpy)-$Ru(bpy)_2^{2+}$ units that are responsible for the observed single-exponential decay kinetics.

The quantum yield (Φ) values for the model compound, G1, G2, and G3 metallodendrimers were 1.5×10^{-3}, 2.1×10^{-2}, 3.0×10^{-2}, and 1.1×10^{-2}, respectively. Interestingly, the observed overall quantum yields of the G1−G3 metallodendrimers are approximately 14, 20, and 7 times that of the quantum yield of the monometallic model complex. The aforementioned steady-state and time-resolved emission study revealed the fact that only one type of emitting excited state (^{3}MLCT) existed in the metallodendrimers with silsesquioxane centers. However, this observation does not exclude the possibility of the formation of additional nonemissive quenching paths as the molecular structure becomes more densely packed in higher generation of dendrimer, which may lower the observed overall quantum yield.

Redox Characteristics. Using cyclic voltammetry, the electrochemical study of the metallodendrimers and the model compound revealed redox waves with formal potentials at ca. +1.36 V (vs SCE, $\Delta E_{1/2} = 60-71$ mV) for the multiple $Ru^{II/III}$ redox couples on dendrimer surface. A representative cyclic voltammogram of the model compound $\{(bpy)_2Ru(tpy)_1$-[G1]-$CH_3\}[PF_6]_2$ is given in Figure 7a. Similar cyclic voltammetric data were obtained for the metallodendrimers as well. Here, the presence of a single reversible $Ru^{II/III}$ redox wave implies simultaneous one-electron processes for the Ru(II) centers on the surface of metallodendrimers.[3b,i] In addition, a lack of significant peak broadening indicates that the ground-state interaction between the peripheral Ru(II) centers is small or nonexistent.[3i,16] The ligand reductions of the model compound (Figure 7a,c), G1, G2, and G3 metallodendrimers (Figure 7e) also exhibit simultaneous processes, which is again indicative of a negligible interaction between the peripheral Ru(II) moieties in the G1−G3 metallodendrimers.

In addition, Figure 7b−e shows evidence of possible film deposition during the continuous potential sweeps. The decrease in current during the anodic sweeps in Figure 7b,d, as well as during the cathodic sweeps in Figure 7c,e, is indicative of film deposition for metal-containing supramolecular systems.[3b,17] Furthermore, the difference in current between the first and successive sweeps is larger in the G3 metallodendrimer (Figure 7d,e) than the model compound (Figure 7b,c), possibly due to an increased film deposition of the much larger metallodendrimer during the continuous potential sweep analysis. Presumably, the film deposition was increased because of the significant difference in the molecular size and the number of ruthenium(II) centers between the metallodendrimers and the much smaller monometallic model compound. Similar current decreases were

(16) Flanagan, J. B.; Margel, S.; Bard, A. J.; Anson, F. C. *J. Am. Chem. Soc.* **1978**, *100*, 4248. (b) Richardson, D. E.; Taube, H. *Inorg. Chem.* **1981**, *20*, 1278−1285.

(17) Takada, K.; Diaz, D. J.; Abruña, H. D.; Cuadrado, I.; Casado, C.; Alonso, B.; Moran, M.; Losada, J. *J. Am. Chem. Soc.* **1997**, *119*, 10763−10773. (b) Denisevich, P.; Willman, K. W.; Murray, R. W. *J. Am. Chem. Soc.* **1981**, *103*, 4727−4737. (c) Abruña, H. D.; Denisevich, P.; Umana, M.; Meyer, T. J.; Murray, R. W. *J. Am. Chem. Soc.* **1981**, *103*, 1−5.

(18) Willman, K. W.; Murray, R. W. *J. Electroanal. Chem.* **1982**, *133*, 211−231. (b) Pickup, P. G.; Kutner, W.; Leidner, C. R.; Murray, R. W. *J. Am. Chem. Soc.* **1984**, *106*, 1991−1998.

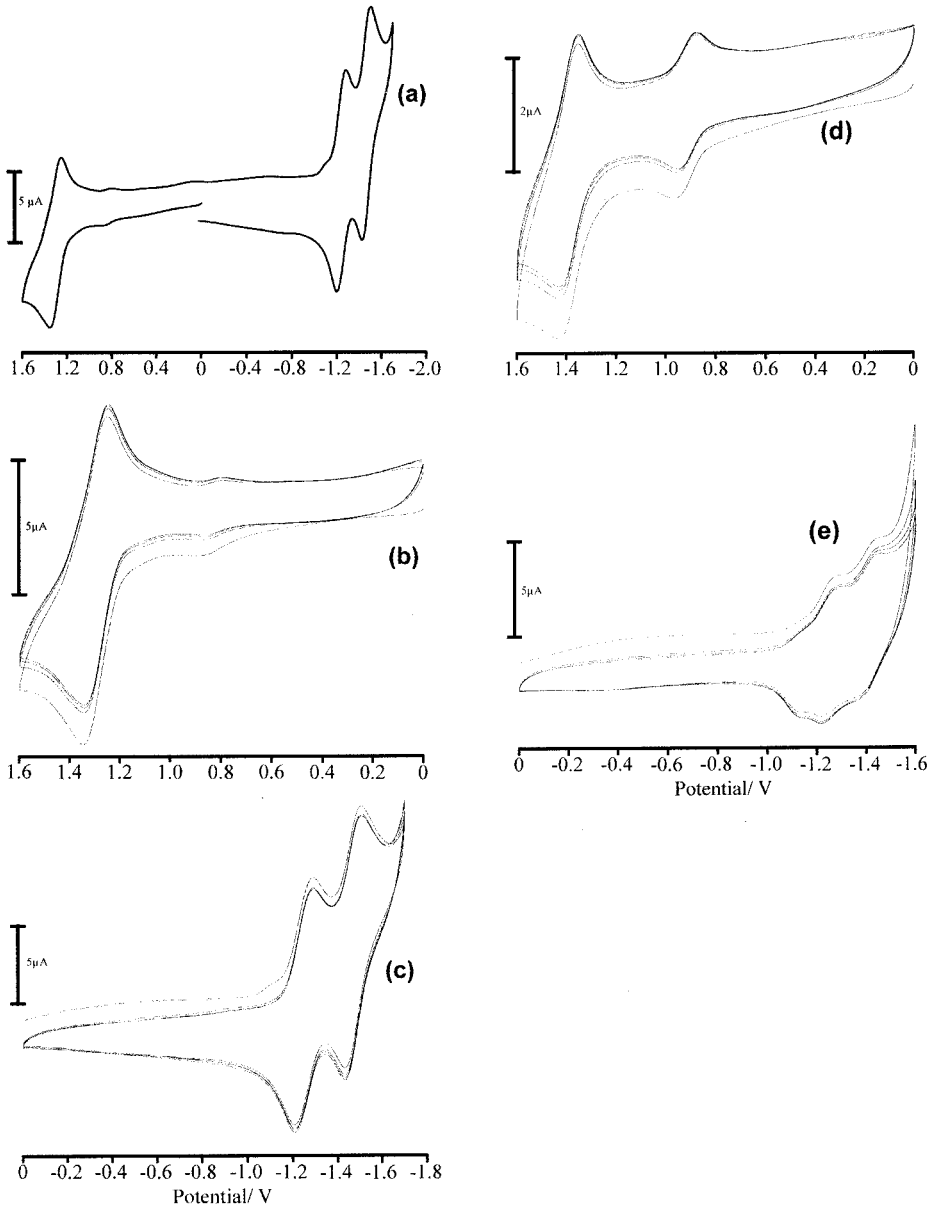

Figure 7. (a−c) Cyclic voltammograms of the model compound, $\{(bpy)_2Ru(tpy)_1\text{-}[G1]\text{-}CH_3\}[PF_6]_2$, and (d−e) cyclic voltammograms of the G3 metallodendrimer, $\{((bpy)_2Ru(tpy))_{32}\text{-}[G3]\text{-}Si_8O_{12}P_8\}[PF_6]_{64}$, in spectrograde acetonitrile (dried over 4 Å molecular sieves) with scan rate 200 mV/s. For more details please see Results and Discussion.

also observed for the G1 and G2 metallodendrimers, and the magnitude of such decrease appeared to be proportional to the generation number of the metallodendrimer.

Figure 7b,d also shows a smaller voltammetric wave with a formal potential of ca. +0.9 V (vs SCE). It was initially suspected that it might correspond to an impurity; however, the ratio between the redox peaks at +0.9 and +1.36 V did not change significantly when repeated column chromatographic separation was applied. Although we have not been able to unambiguously identify the origin of this redox wave at +0.9 V, a similar observation of a smaller redox peak from a surface-confined species was reported for the polyamidoamine dendrimer with multiple terminal bis(terpyridyl)ruthenium(II) groups.[3b] Hence, it is possible that the additional redox wave at +0.9 V may also be caused by surface-confined species for the G1−G3 metallodendrimers. In addition, the relative magnitude of this redox couple in the model compound (Figure 7b) is much smaller than in the G3 metallodendrimer (Figure 7d), and the peak height of this redox couple also increases upon going from the G1 to G3 metallodendrimer. These surface-confined redox species might be created during the applied anodic potential sweeps (0−1.6 V), where charges were trapped in a "microdomain" on the electrode surface. For the G3 metallodendrimer, significantly more of this species was produced during the first anodic sweep and remained until it could be discharged during the cathodic sweep.

Conclusion

We have shown that the surface-modified "starburst" dendrimers were prepared by attaching terpyridine-terminated polyether monodendrons to an octafunctionalized silsesquioxane core through phosphonium linkage groups. Surface-modified organic dendrimers with 8, 16, and 32 peripheral terpyridine groups have been synthesized. Further surface complexation of these dendrimers with an appropriate Ru(II) starting material yielded the corresponding spherically shaped metallodendrimers that featured 8, 16, and 32 photoactive and redox-active chromophores. Room-temperature luminescence at 605−611 nm was observed for the G1−G3 metallodendrimers and the model compound. These metallodendrimers exhibited chromophore

summation effects in the electronic absorption measurements, with ligand-centered (LC) charge transfer and metal-to-ligand charge transfer (MLCT) bands at 288 nm and 455 nm, respectively. Single-exponential excited-state decay kinetics were observed for the G1−G3 metallodendrimers, which suggested negligible intramolecular interaction between the multiple surface-confined Ru(II)-based chromophores. Electrochemical characterization of the G1−G3 metallodendrimers displayed evidence of surface-confined species. These surface-confined species may create charge-trapped microdomains between the inner deposited layer and an outer layer during the subsequent potential sweeps, which manifested themselves as current prepeaks to the redox waves of the inner layer films.

Acknowledgment. This work was supported by the National Science Foundation and the California Energy Institute EST Program. We thank Prof. Frank J. Feher (UC Irvine) for the silsesquioxane starting material, [G0]-$Si_8O_{12}P_8$.

IC000490W